JACS
JOURNAL OF THE AMERICAN CHEMICAL SOCIETY
Article
pubs.acs.org/JACS

Mechanism of Ion Permeation and Selectivity in a Voltage Gated Sodium Channel

Ben Corry*,† and Michael Thomas†

School of Biomedical, Biomolecular and Chemical Sciences, The University of Western Australia, Crawley, WA 6009 Australia

Supporting Information

ABSTRACT: The rapid and selective transport of Na^+ through sodium channels is essential for initiating action potentials within excitable cells. However, an understanding of how these channels discriminate between different ion types and how ions permeate the pore has remained elusive. Using the recently published crystal structure of a prokaryotic sodium channel from *Arcobacter butzleri*, we are able to determine the steps involved in ion transport and to pinpoint the location and likely mechanism used to discriminate between Na^+ and K^+. Na^+ conduction is shown to involve the loosely coupled "knock-on" movement of two solvated ions. Selectivity arises due to the inability of K^+ to fit between a plane of glutamate residues with the preferred solvation geometry that involves water molecules bridging between the ion and carboxylate groups. These mechanisms are different to those described for K^+ channels, highlighting the importance of developing a separate mechanistic understanding of Na^+ and Ca^{2+} channels.

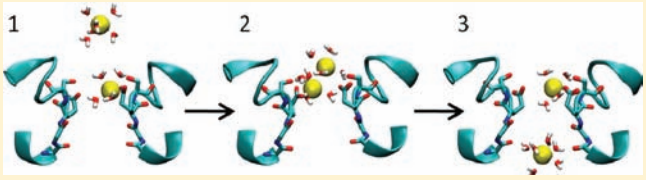

INTRODUCTION

The rapid passage of Na^+ and K^+ into and out of excitable cells through separate selective pathways underlies the generation and regulation of electrical signaling in living organisms.[1,2] Studies of the detailed mechanisms of ion transport and selectivity in sodium selective channels has been hampered by a lack of structural information, and so recently the focus of understanding the molecular basis of transport and selectivity has been on the family of K^+ selective channels for which atomistic information is available.[3] Although there have beenmany studies examining the steps involved in ion permeation in potassium channels[4−7] and rigorous debate continues as to the basis of ion discrimination in these,[8−13] in the case of sodium channels the steps involved in ion permeation and the mechanism of discrimination between Na^+, K^+, and Ca^{2+} wait to be determined. Early pore models by Hille explained how large organic cation could be excluded by a pore of a particular size but could not explain the discrimination between smaller partly hydrated ions.[14] Instead, the field strength concepts of Eisenman[15] have been suggested to play a role in selectivity, as the selectivity sequence is similar to that expected in a high field strength binding site that could be created by the pore lining residues provided certain geometrical constraints are also at play.[14,16] Similar concepts have been discussed with regard to ion discrimination in potassium channels where the importance of the chemical nature of the pore lining atoms and the various structural restraints placed upon them continue to be discussed. How the sodium channel discriminates between Na^+, K^+, and Ca^{2+} is not yet clear.

The recent exciting publication of the crystal structure of a prokaryotic homotetrameric voltage gated sodium channel NavAb from *Arcobacter butzleri*[17] has opened the door for these questions to be answered. The topography of the pore forming region of NavAb is similar to the familiar topography of the pore forming region of potassium channels. The S6 helices form an inverted tepee that lines the inner half of the pore and a re-enterant loop forms the narrow external section of the pore known from mutation studies to be responsible for creating ion selectivity.[18,19] The detailed structure of the narrow 'selectivity filter' is, however, significantly different to that of potassium channels, being both wider and shorter as well as being partly lined by amino acid side chains as shown in the inset to Figure 1. The external end of the filter is surrounded by side chains of four glutamate residues (Glu177) from each of the four protein chains, forming an "EEEE" ring in the same sequence position as the characteristic DEKA ring found in eukaryotic sodium channels.[17] In this manuscript we use this crystal structure as the starting point for molecular dynamics simulations to study the steps involved in ion permeation and the mechanisms by which ion selectivity is achieved.

SIMULATION DETAILS

Protein coordinates were obtained from the protein database, PDB accession code 3RVY.[17] In order to conduct the molecular dynamics simulations, the protein was placed in a pre-equilibrated POPC lipid bilayer, solvated in a 115 × 115 × 90 Å box of TIP3P water with 300 mM NaCl. An ion concentration at the large end of physiological values is used so as to better screen the electrostatic influence of the protein in the neighboring periodic simulation shell. The protein was initially held fixed while the lipid and water were allowed to equilibrate for 1.5 ns, before the protein alpha carbons were restrained with a harmonic potential of force constant decreasing from 1 to 0.01 kcal/mol in 6 steps each lasting 0.6 ns. To account for the lipid molecules protruding into the center of the pore in the crystal structure, the tails

Received: November 2, 2011
Published: December 15, 2011

dx.doi.org/10.1021/ja210020h | J. Am. Chem.Soc. 2012, 134, 1840−1846

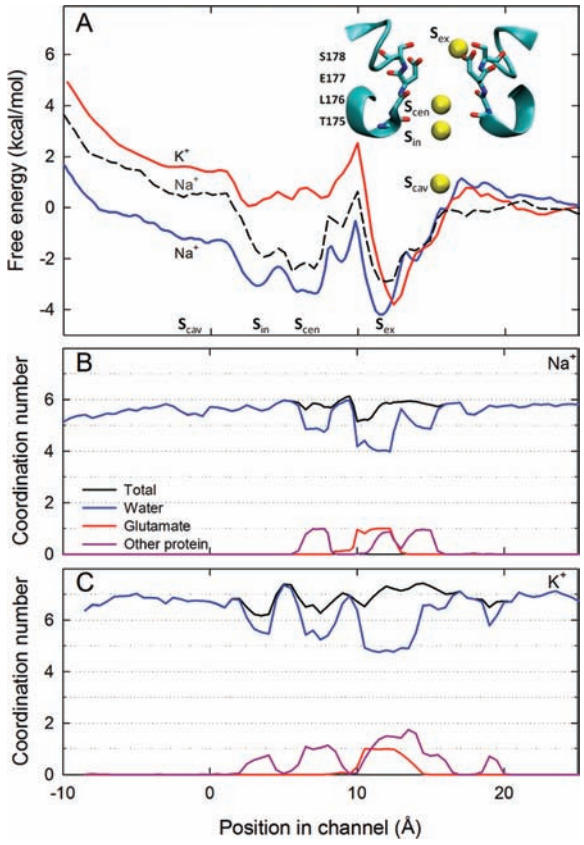

Figure 1. Single ion potential of mean force (PMF) and ion coordination numbers in the pore. (A) The single ion PMF is shown for Na^+ (blue) and K^+ (red) as a function of the axial position in the pore. The profile for Na^+ in a channel in which one of the four Glu177 residues is protonated is also shown (dashed line). The coordination numbers are indicated for (B) Na^+ and (C) K^+ as a function of position in the pore. The total coordination number is shown in black, while the contribution from water (blue), glutamate side chains (red) and other protein residues (purple) are indicated. The chemical nature of the selectivity filter as well as the ion binding sites labeled $\mathbf{S}_{ex}$, $\mathbf{S}_{cen}$, $\mathbf{S}_{in}$, and $\mathbf{S}_{cav}$ are shown in the inset.

of four lipid molecules were restrained to the crystallographic positions with a force constant slowly increasing during the period in which the protein was fixed. During data collection they were restrained with a force constant of 0.1 kcal/mol/Å^2.

Potentials of mean force (PMF) were calculated using umbrella sampling[20] with either one or two ions harmonically restrained in 0.5 Å steps in the axial (z) direction with a force constant of 5 kcal/mol/Å^2. Collective analysis was made with the weighted histogram analysis method[21] using the implementation of Grossfield.[22] To reduce the amount of equilibration time required in each umbrella window, a number of starting coordinates were generated in which one or two ions were swapped with equilibrated water molecules throughout the length of the pore. In the two ion case, this meant starting coordinates were generated with the ions separated by integer numbers of water molecules. Prior to all simulations the test ion(s) was held fixed for 10 ps to allow water to equilibrate around it. Each single ion PMF involves 71 simulations each lasting 1 ns, with the first 0.5 ns used as equilibration. Each two ion PMF was made from ~2000 windows each lasting 0.2 ns with the first 0.1 ns excluded as equilibration. Thus a complete two ion PMF required 400 ns of simulation.

Unless otherwise stated, all simulations were conducted using the CHARMM27 force field for the protein, water and lipid;[23] ion parameters from Joung;[24] using NAMD[25] with periodic boundary conditions, a 1 fs time step at constant pressure (1 atm) and temperature (298 K). A harmonic potential of 0.01 kcal/mol/Å^2 was held on the α-carbon atoms, except for those forming the selectivity filter (residues 174–183) during data production. Coordination numbers were defined as the number of non-hydrogen atoms within 3.0 and 3.4 Å of Na^+ and K^+ respectively, the positions of the first minimum in the bulk ion-water oxygen radial distribution function.

RESULTS AND DISCUSSION

To understand ion permeation in the channel we calculate single and multi-ion free energy profiles in the pore that have been beneficial in understanding permeation in K^+ channels.[5,7,26,27] As may be expected from the presence of the negatively charged glutamate residues, the single ion potential of mean force (PMF) shown in Figure 1A indicates that Na^+ is attracted from the external solution and can be expected to bind near the external end of the filter in the site labeled $\mathbf{S}_{ex}$. In this position the ion sits off axis where it can be directly coordinated by one of the four glutamates as well as the side chain of Ser178 and four water molecules as shown in Figure 1B and pictured in Figure 2. The coordination structure of the

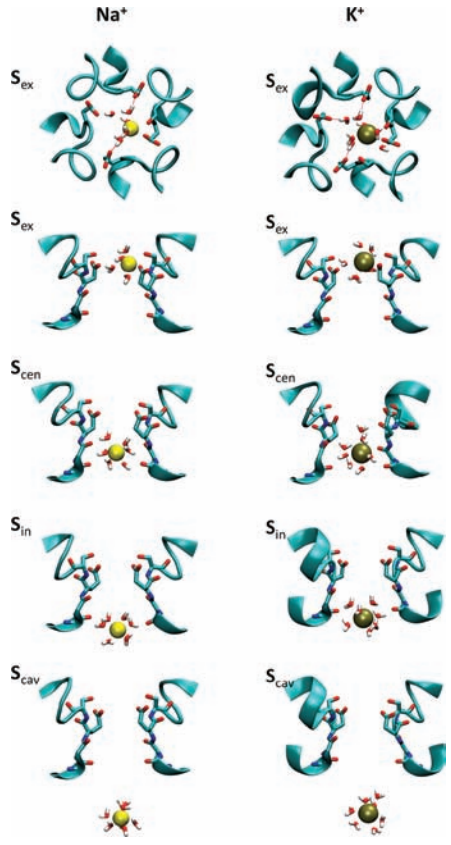

Figure 2. Ion binding sites. Snapshots of Na^+ (left column) and K^+ (right column) in each of the ion binding sites are shown along with the water molecules directly coordinating the ion. A top view is given for the site $\mathbf{S}_{ex}$ only.

ion in the site is influenced by the other three Glu177 residues, with two of the water molecules coordinating the ion also forming hydrogen bond donors to the glutamate side chains as had been predicted.[14,17] Na^+ experiences an energy barrier of 4 kcal/mol to leave the external site and move into the channel, and two additional binding sites ($\mathbf{S}_{cen}$ and $\mathbf{S}_{in}$) are evidenced by the energy wells toward the inner end of the filter. In these positions the ion is coordinated by an entire hydration shell which loosely interacts with the polar pore lining as seen in

dx.doi.org/10.1021/ja210020h | J. Am. Chem.Soc. 2012, 134, 1840–1846

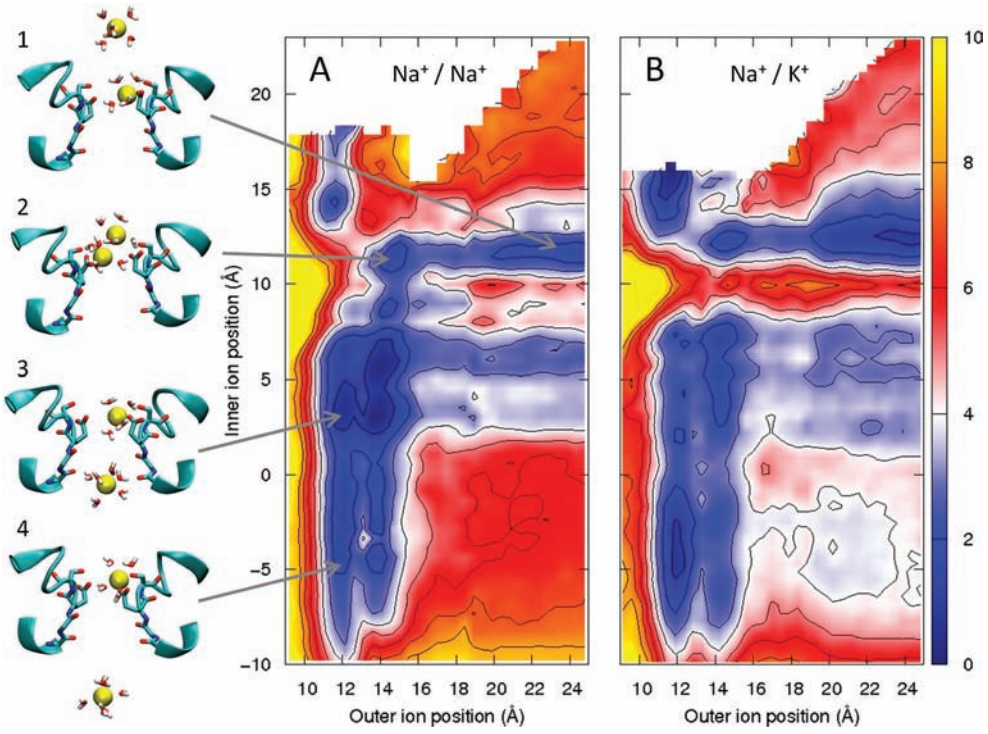

Figure 3. Two ion energy profiles and conduction mechanism. The PMF is plotted as a function of the axial position of each ion assuming (A) both ions are Na^+, and (B) the inner ion is K^+ and the outer ion is Na^+. Energy values are shown in scale bar in units of kcal/mol and the contour interval is 1 kcal/mol. The steps involved in conduction and their positions on the 2 ion PMF are shown on the left. A movie showing the steps involved in Na^+ conduction through the pore in which the pore lining section of two of the four protein chains are shown along with the side chains of two Glu177 residues and the hydration shell of each ion is available in the HTML version.

Figure 2 and suggested by Payandeh et al.[17] The calculations described so far assume that all four glutamate residues are deprotonated and carry a net negative charge. It may be possible that one or more of these is protonated at physiological pH as is suspected in voltage gated calcium channels that share a ring of four nearby glutamate residues.[28,29] To account for this possibility, an additional single ion PMF for Na^+ was calculated with one of the glutamate residues protonated (dashed line Figure 1A). Although the depth of the external well is less, the same binding sites and energy barrier are present.

Although it may be possible for a single ion to overcome the 4 kcal/mol energy barrier to enter the inner binding sites on its own, this process could be sped up by the presence of additional ions. To investigate this we calculated the free energy landscape in the presence of two ions as shown in Figure 3A. From this plot, a mechanism of Na^+ conduction becomes immediately apparent. The first ion to enter the pore is likely to bind at the external site $\mathbf{S}_{ex}$ (Figure 3, inset 1). A second ion is weakly attracted to the pore and can approach very close to the first ion where there is a small energy minimum (inset 2). At this point the energy barrier for the first ion to move into one of the internal sites is small (~2.5 kcal/mol), and when this ion moves into the pore, the second ion moves into $\mathbf{S}_{ex}$ (inset 3). From this point the inner ion can easily move into the central cavity (inset 4). Motion further into the channel cannot be investigated due to the channel being closed at the internal end. Movement of a sodium ion from the external solution to the central cavity has a maximum energy barrier of 2−3 kcal/mol, in the right order of magnitude to produce the large fluxes measured in the pore,[30] and similar barrier to those seen for K^+ in potassium channels.[5] There is some controversy in the literature as to the number of ions expected to be involved in conduction in eukaryotic sodium channels. Measurements of unidirectional fluxes have been taken to suggest only a single ion is required for conduction,[31,32] but stochastic simulations have shown the flux measurements are consistent with a multi-ion conduction mechanism[33] as suspected from the non-independence of ion movement[34] and factors such as Li^+ block.[14]

While this two ion transport mechanism can be described as "knock-on" conduction in which the presence of a second ion aids the first to move through the pore, it is distinctly different to that taking place in potassium channels. Although a single ion could permeate on its own, the presence of the second ion assists conduction as evidenced by the larger barrier and lack of an energy well for the inner ion in the cavity when the second ion remains in bulk (right-hand edge of Figure 3A). However, the two ions in the pore move sequentially (although not independentally as described above), with one ion moving while the other remains in roughly the same position. This is evidenced by all the steps in conduction involving either horizontal or vertical motion on the free energy plot, a process we term 'loosely coupled knock on conduction'. In contrast, conduction in potassium channels requires the simultaneous motion of two or more ions.[4,5] The different behavior of ions in the two channels is partly a consequence of the different widths of the pores. In the wider sodium channel, when one ion moves, water can move around it to replace it in the pore. In the narrower potassium channel there is no space for ions and water to exchange positions and the ions and water must move in single file. Ions also move through the sodium channel with the first hydration shell intact as seen in the plot of coordination numbers (Figure 1B) and pictured in Figure 2

dx.doi.org/10.1021/ja210020h | J. Am. Chem.Soc. 2012, 134, 1840−1846

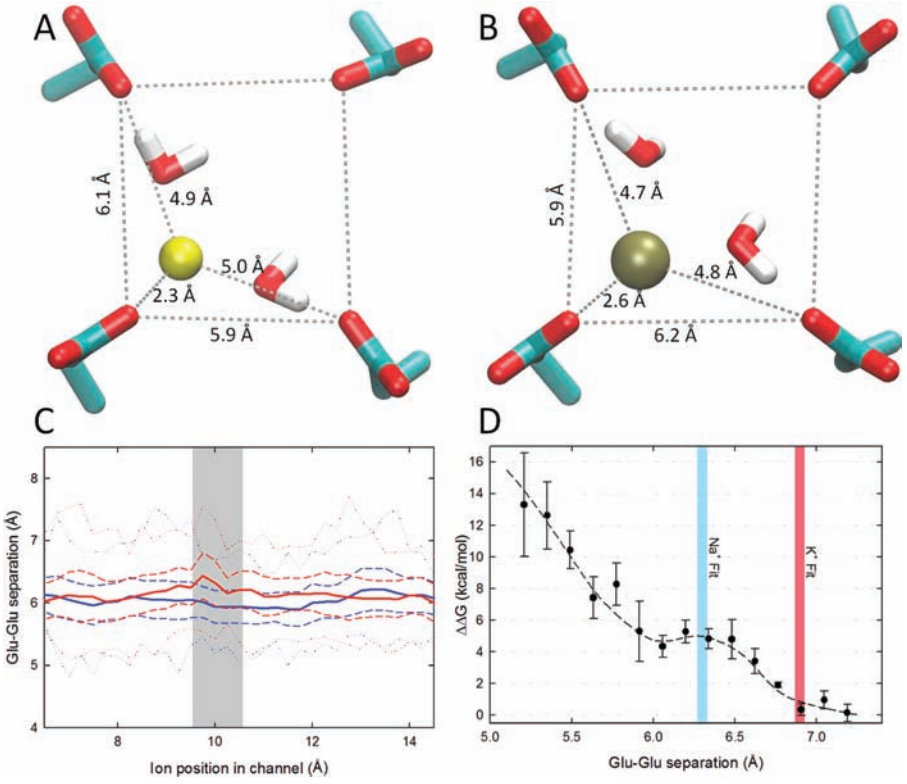

Figure 4. Mechanism of ion selectivity. Snap shots of (A) Na^+ and (B) K^+ at the transition point in the plane of the glutamate side chains are shown along with the side chains themselves and two of the water molecules hydrogen bonded to them that also coordinate the ion. Dimensions of the system are shown and it is apparent that the water can sit in a direct line between the carboxylate group and the ion for Na^+ but not for K^+. (C) The average Glu177−Glu177 distance measured between the inward pointing carboxylate oxygens is plotted against the position of the ion in the channel. The average distance is shown in solid lines for Na^+ (blue) and K^+ (red). The standard deviation is indicated by the dashed lines and the maximum and minimum values by the dotted lines. The region corresponding to the ion sitting in the plane of the side chains is highlighted by the gray box. (D) Relationship between selectivity and pore radius in a model pore. The difference in free energy for K^+ to pass through plane of the glutamates side chains relative to Na^+ is shown for model pores of various sizes created from the residues forming the selectivity filter of NavAb. The pore size required for Na^+ and K^+ to fit in plane with the glutamate side chains along with two water molecules are shown by the blue and red bars respectively.

as had previously been suspected,[14,17] while the narrow potassium channel pore requires near complete dehydration. In this case there is also enough space for ions to move around each other in the external site $\mathbf{S}_{ex}$ (Figure 3A), reducing the chance of block or current attenuation.

To examine how the protein discriminates between Na^+ and K^+ we show energy profiles in the presence of K^+. The single ion profile for K^+ (Figure 1A) is similar to that for Na^+, with both the external ($\mathbf{S}_{ex}$) and internal binding sites ($\mathbf{S}_{cen}$ and $\mathbf{S}_{in}$) visible. Notably, however, there is a larger barrier for a single K^+ to move between $\mathbf{S}_{ex}$ and $\mathbf{S}_{cen}$ than was the case for Na^+. In all these binding sites, K^+ maintains a large coordination number similar to that seen in bulk in the simulations; it binds to one Glu 177, one or two Ser178 side chains and 4 or 5 water molecules in $\mathbf{S}_{ex}$, while being surrounded by 6 or 7 waters in $\mathbf{S}_{cen}$ and $\mathbf{S}_{in}$ (Figures 1C and 2). The barrier for K^+ to move between $\mathbf{S}_{ex}$ and $\mathbf{S}_{cen}$ becomes more apparent when we examine the two ion PMF shown in Figure 3B, which plots the free energy in the presence of one K^+ (internal ion) and one Na^+ (external ion). Whereas the barrier for the internal ion to move between $\mathbf{S}_{ex}$ and $\mathbf{S}_{cen}$ is lowered when two Na^+ are in the channel, the same is not the case when K^+ is in the inner position. The lowest energy pathway for this ion to enter the inner binding sites is 5−6 kcal/mol whether a second ion is present or not. A similar energy barrier is seen in the PMF created with two K^+ ions, while a small barrier is seen when Na^+ is the inner ion and K^+ the outer ion (Figure S1) highlighting that it is the nature of the inner ion that dictates the barrier to ion conduction. The energetic differences between Na^+ and K^+ are less (3 kcal/mol) than seen in K^+ channels (~6 kcal/mol)[7] consistent with the much lower selectivity (10 to 30 fold) measured in Na^+ channels.[14,17,19]

Surprisingly, ion selectivity does not arise at the binding site $\mathbf{S}_{ex}$ where the ion directly contacts one of the glutamate and one serine residue, as both Na^+ and K^+ can be seen to bind with similar affinity at this position. Previous studies have suggested that the presence of highly charged ligands in an ion binding site may be enough to create ion selectivity.[15,35,36] However, this does not occur in this site, most likely due to the space available around the ion which allows for significant flexibility in the number and orientation of water molecules that can surround each ion. It can also be seen from Figure 3B that Na^+ can pass K^+ bound at the external site and is more likely to penetrate the pore than the resident K^+.

Both the single ion and two ion free energy surfaces show that ion selectivity arises at the saddle point at roughly z = 10 Å where the ions have to pass through the plane of the four Glu177 side chains. Discrimination between Na^+ and K^+ could arise for many reasons, but most of these do not apply in this case. The pore is too wide to separate the ions based upon the

dx.doi.org/10.1021/ja210020h | J. Am. Chem.Soc. 2012, 134, 1840−1846

bare ion size. A plot of the coordination numbers of the ions (Figure 1) also shows that both Na^+ and K^+ can pass through the channel with favorable numbers of surrounding ligands (mostly water) and this is nearly constant at all positions in the channel, meaning that the enforcement of specific coordination numbers cannot create selectivity here as has been discussed in relation to other proteins.[37−41] A further possibility is that the size of the pore allows for Na^+ to pass with a complete hydration shell, but that K^+ requires partial dehydration.[42] But, again the plot of coordination numbers shows that this is not the case here as K^+ maintains a complete coordination shell at the point of discrimination. The strength of interaction between the ion and the directly coordinating glutamate could aid selectivity in line with the field strength arguments of Eisenman; however, this effect is expected to be small given the limited selectivity at the external site $\mathbf{S}_{ex}$.

A possible reason for the differing energy barriers for Na^+ and K^+ is apparent from careful analysis of the simulation trajectories. A snapshot of the system with each ion type at the transition point, is given in Figure 4A,B. As noted previously, ions bound near the four glutamate residues like to directly coordinate to one of the side chains while two water molecules can form bridges to two others. An ideal geometry would arise when the bridging water sits in a direct line between the ion and the carboxylate oxygen, as occurs for both ion types in the energy minima at $\mathbf{S}_{ex}$. However, when the ion moves into the plane of the glutamates the limited space available means that it is more difficult for the bridging water molecules to adopt this ideal geometry. Simple geometric analysis shows that unless the Glu177 side chains can move significantly outward in the presence of K^+, this ion will not fit in plane with the bridging waters. This is because the ion-Glu177 distance required to allow bridging is larger for K^+ than for Na^+ (~5.4 Å compared to 5.0 Å) while the available space is smaller for K^+ as it sits further from the directly coordinating side chain. As a consequence the bridging water molecules have to sit in a less favorable position in the presence of K^+, out of the direct line as seen in Figure 4B, creating a preference for Na^+ in the channel. This mechanism requires that the Glu177 side chains are not completely free to move outward from the pore in the presence of K^+. It was noted in the crystal structure that the oxygen of the Glu177 carboxylate group pointing away from the pore accepts a hydrogen bond from the backbone amide of both Ser 1180 and Met 1181.[17] This is also seen throughout the simulations and together with direct attraction to the permeating ion could limit the amount of radial movement of the side chain. However, the proposed mechanism for generating selectivity does not require precise positioning of the glutamate side chains. Analysis of the simulation data shows that the side length of the square formed by the four inward pointing carboxylate oxygens fluctuates significantly (by over 1 Å) but is only slightly larger when K^+ sits in the plane than for Na^+ (Figure 4C). The difference is not as large as the 0.6 Å required to achieve similar bridging for the two ions.

The explanation of selectivity presented here requires both a pore of roughly the correct size and the presence of carboxylate groups to form strong hydrogen bonds to the bridging water (Figure 5), and so two testable consequences follow. First, removing the charge on the glutamate side chains is found to remove selectivity in the simulations while maintaining the size of the pore. This confirms the importance of the chemical nature of the carboxylates and that it is not the size of the pore alone that creates selectivity.

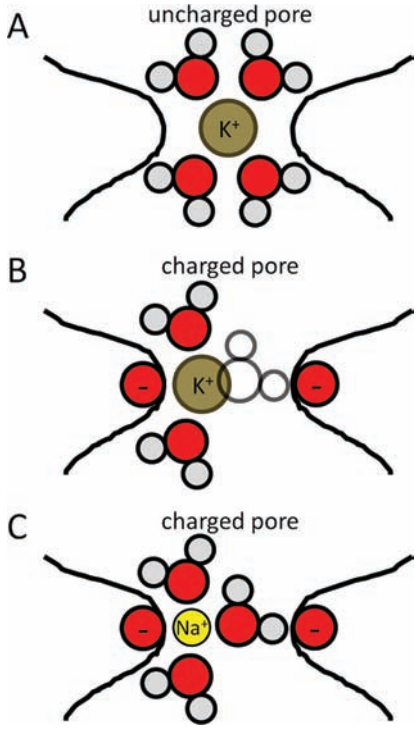

Figure 5. Schematic depiction of the proposed mechanism of ion selectivity in NavAb. Although K^+ could fit through the narrow portion of the pore with a complete hydration shell as shown in (A), it cannot do so with the geometry preferred in the presence of the charged glutamate residues (B) which involves water molecules bridging between the ion and the nearby glutamate side chains. In contrast, the smaller Na^+ ion can fit through the pore with the preferred geometry (C).

Second, widening the ring of glutamates through an enforced harmonic constraint on the Glu177 C_α that increases the average side length of the glutamate square by 0.2 Å, decreases the selectivity from 3.0 to 1.5 kcal/mol. This effect can be tested in a more controlled manner by examining how the selectivity is influenced by the pore radius in a model system. To do this we create pores of different radii using residues 1175−1179 that form the selectivity filter. Each pore model is placed in a cylindrically restrained column of water as illustrated in Figure S2 and the PMF involved in moving a single ion through the pore was determined using umbrella sampling while restraining the protein atoms with a strong harmonic potential. In Figure 4D we plot the difference in free energy for K^+ to move through the plane of the Glu177 side chain relative to the energy minima in site $\mathbf{S}_{ex}$ compared to that for Na^+. In the wide pores there is little discrimination between the ions, but selectivity for Na^+ is found once the pore can no longer accommodate bridging water molecules in plane with K^+. The plateau in selectivity seen when the glutamate separation is around 6.3 Å is centered on the size at which Na^+ can optimally fit in the pore with 2 bridging water molecules. Although the degree of selectivity is slightly higher in the model than in the simulations of the full protein (most likely due to the stronger restraints on the protein position), these results highlight that selectivity in this pore does not require precise positioning of the side chains and a similar degree of selection could be expected across a range of pore sizes. Although a greater degree of selectivity is found in the narrower pore sizes (as additional water molecules must be stripped from K^+ and due to

dx.doi.org/10.1021/ja210020h | J. Am. Chem.Soc. 2012, 134, 1840−1846

increasing field strength of the site due to closeness of the neighboring acidic side chains) there are also larger energy barriers for both ions to pass through the pore which would reduce the ion flux.

While most of the tests of our hypothesis for how selectivity arises in the pore described above are computational, there are some situations that can be probed experimentally. Mutating the Glu177 ring, for example, is likely to have a large affect of the function of the channel. As shown in Figure S3, removing the charge on the residues as in the Glu177Ala mutation, removes the strong ion binding in the pore and can be expected to render it nonconductive unless a substantial structural change occurs. The more subtle Glu177Asp mutation, on the other hand, is found to increase the affinity of ion binding. Due to the orientation of the side chain which points along the length of the pore (Figure 3), shortening it does not increase the width of the pore. In addition, this mutation removes the hydrogen bond between the side chain and Ser1180/Met1181 allowing more freedom to the carboxylate group, and for the ions to coordinate to two side chains simultaneously.

A change in protonation state of the Glu177 side chains (which may be elicited by a change in pH) could also affect ion permeation. As can be seen in Figure S4, the protonation of a single side chain yields similar single ion PMFs and only a very small decrease in selectivity. This also strengthens the plausibility of our explanation of selectivity given the uncertainty in the protonation state of the residues. Protonating two of the side chains, however, has a much larger effect. Not only does this prevent the kind of ion/water binding geometries pictured in Figure 4A,B, but also the reduced electrostatic attraction appears to remove the affinity of the selectivity filter for either ion.

The choice of parameters for the ions is one of the most difficult aspects of nonpolarizable force field calculations as it is difficult to reproduce both solvation energies and structures using such a simple model. To test the uncertainty this can introduce into our results we recalculated the single ion PMFs for both Na^+ and K^+ using the 'standard' CHARMM ion parameters developed by Beglov and Roux as seen in the Figure S5. Although this highlights that sub kcal/mol energies are beyond the accuracy of the model, the result is very similar to those obtained with the parameters of Joung and Cheatham[24] suggesting the robustness of the trends reported above.

CONCLUSION

The elucidation of the first atomic resolution structure of a sodium selective channel provides a fascinating glimpse into the functioning of this class of ion channel. Studying the energetics of ion permeation in NavAb has shown a multi-ion conduction mechanism that is different to that seen in potassium channels involving independent movements of solvated ions. More intriguingly, selectivity between Na^+ and K^+ is shown to result from a combination of the chemical nature of the pore lining and the size of the pore in the plane of the Glu177 side chains. Although K^+ could fit through the pore with a complete hydration shell, it cannot do so with the geometry preferred in the presence of the charged glutamate residues as illustrated in Figure 5. This concept couples many of the geometric arguments of Hille[14] with the field strength concept of Eisenmann[15] and shows how the geometrical arrangement of ions and water in the pore can influence ion discrimination. Eukaryotic voltage gated sodium channels do not contain the ring of glutamates shown to be important here but rather the DEKA motif, and it remains to be seen if the geometric basis of selectivity described here could apply with a change in the chemical environment, especially given the suggestion that the lysine residue is critical in maintaining the rigidity and size of the pore.[43]

ASSOCIATED CONTENT

Supporting Information

Two-ion free energy surfaces for additional ion combinations and a depiction of the model system used to produce Figure 4D. This material is available free of charge via the Internet at http://pubs.acs.org.

Web-Enhanced Feature

A movie showing the steps involved in Na^+ conduction through the pore in which the pore lining section of two of the four protein chains are shown along with the side chains of two Glu177 residues and the hydration shell of each ion is available in the HTML version.

AUTHOR INFORMATION

Corresponding Author

*ben.corry@uwa.edu.au

Present Address

[†]Research School of Biology, The Australian National University, Canberra, ACT 0200, Australia.

ACKNOWLEDGMENTS

This work was supported by computer time from the Pawsey Centre Project in Western Australia and research funding from the Australian Research Council.

REFERENCES

(1) Hille, B. *Ionic Channels of Excitable Membranes*, 3rd ed.; Sinauer Associates Inc.: Sunderland, MA, 2001.
(2) Catterall, W. *Neuron* **2000**, *26*, 13−25.
(3) Doyle, D. A.; Morais Cabral, J.; Pfuetzner, R. A.; Kuo, A.; Gulbis, J. M.; Cohen, S. L.; Chait, B. T.; MacKinnon, R. *Science* **1998**, *280*, 69−77.
(4) Åqvist, J.; Luzhkov, V. *Nature* **2000**, *404*, 881−884.
(5) Bernèche, S.; Roux, B. *Nature* **2011**, *414*, 73−77.
(6) Khalili-Araghi, F.; Tajkhorshid, E.; Schulten, K. *Biophys. J.* **2006**, *91*, L72−L74.
(7) Jensen, M. O.; Borhani, D. W.; Lindorff-Larsen, K.; Maragakis, P.; Jogini, V.; Eastwood, M. P.; Dror, R. O.; Shaw, D. E. *Proc. Natl. Acad. Sci. U.S.A.* **2010**, *107*, 5833−5838.
(8) Alam, A.; Jiang, Y. *J. Gen. Physiol.* **2011**, *137*, 397−403.
(9) Nimigean, C.; Allen, T. *J. Gen. Physiol.* **2011**, *137*, 405−413.
(10) Roux, B.; Bernèche, S.; Egwolf, B.; Lev, B.; Noskov, S. Y.; Rowley, C. N.; Yu, H. *J. Gen. Physiol.* **2011**, *317*, 415−426.
(11) Dixit, P. D.; Asthagiri, D. *J. Gen. Physiol.* **2011**, *137*, 427−433.
(12) Varma, S.; Rogers, D.; Pratt, D.; Rempe, S. *J. Gen. Physiol.* **2011**, *137*, 479−488.
(13) Fowler, P. F.; Tai., K.; Sansom, M. S. P. *Biophys. J.* **2008**, *95*, 5062−5072.
(14) Hille, B. *J. Gen. Physiol.* **1972**, *59*, 637−658.
(15) Eisenman, G. *Biophys. J.* **1962**, *2*, 259−323.
(16) Chandler, W. K.; Meves, H. *J. Physiol.* **1965**, *180*, 788−820.
(17) Payandeh, J.; Scheuer, T.; Zheng, N.; Catterall, W. *Nature* **2011**, *475*, 353−358.
(18) Heinemann, S.; Terlan, H.; Stühmer, W.; Imoto, K.; Numa, S. *Nature* **1992**, *356*, 441−443.
(19) Favre, I.; Moczydlowski, E.; Schild, L. *Biophys. J.* **1996**, *71*, 3110−3125.
(20) Torrie, G.; Valleau, J. *Chem. Phys. Lett.* **1974**, *28*, 578−581.

(21) Kumar, S.; Bouzida, D.; Swendsen, R.; Kollman, P.; Rosenberg, J. *J. Comput. Chem.* **1992**, *13*, 1011−1021.
(22) Grossfield, A. *An implementation of WHAM: the Weighted Histogram Analysis Method.* http://membrane.urmc.rochester.edu/Software/WHAM/WHAM.html (accessed 26/1/2010).
(23) MacKerell, A. D. Jr.; et al. *J. Phys. Chem. B.* **1998**, *102*, 3586−3616.
(24) Joung, I. S.; Cheatham, T. E. III *J. Phys. Chem. B.* **2008**, *112*, 9020−9041.
(25) Phillips, J. C.; Braun, R.; Wang, W.; Gumbart, J.; Tajkhorshid, E.; Villa, E.; Chipot, C.; Skeel, R. D.; Kalé, L.; Schulten, K. *J. Comput. Chem.* **2005**, *26*, 1781−1802.
(26) Egwolf, B.; Roux, B. *J. Mol. Biol.* **2010**, *401*, 831−842.
(27) Furini, S.; Domene, C. *Biophys. J.* **2011**, *101*, 1623−1631.
(28) Root, M. J.; MacKinnon, R. *Science* **1994**, *265*, 1852−1856.
(29) Corry, B.; Allen, T. W.; Kuyucak, S.; Chung, S. H. *Biophys. J.* **2001**, *80*, 195−214.
(30) Hartshorne, R. P.; Keller, B. U.; Talvenheimo, J. A.; Catterall, W. A.; Montal, M. *Proc. Natl. Acad. Sci. U.S.A.* **1985**, *82*, 240−244.
(31) Begenisich, T.; Busath, D. *J. Gen. Physiol.* **1981**, *77*, 489−502.
(32) RakowskiR.GadsbyD.WeerP. D.J. Gen. Physiol.2002
(33) Vora, T.; Corry, B.; Chung, S. H. *Eur. Biophys. J.* **2008**, *38*, 45−52.
(34) Begenisich, T.; Cahalan, M. *J. Physiol.* **1980**, *307*, 243−257.
(35) Noskov, S.; Roux, B. *Nature* **2004**, *431*, 830−834.
(36) Thomas, M.; Jayatilaka, D.; Corry, B. *Biophys. J.* **2011**, *100*, 60−69.
(37) Thomas, M.; Jayatilaka, D.; Corry, B. *Biophys. J.* **2007**, *93*, 2635−2643.
(38) Varma, S.; Rempe, S. *Biophys. J.* **2007**, *93*, 1093−1099.
(39) Bostick, D. L.; Brooks, C. L. III *Proc. Natl. Acad. Sci. U.S.A.* **2007**, *104*, 9260−9265.
(40) Asthigiri, D.; Dixit, P. D.; Merchant, S.; Paulaitis, L. R.; Rempe, S. B.; Varma, S. *Chem. Phys. Lett.* **2010**, *485*, 1−7.
(41) Dixit, P. D.; Merchant, S.; Asthigiri, D. *Biophys. J.* **2009**, *96*, 2138−2145.
(42) Song, C.; Corry, B. *J. Phys. Chem. B* **2009**, *113*, 7642−7649.
(43) Dudev, T.; Lim, C. *J. Am. Chem. Soc.* **2010**, *132*, 2321−2332.